Synthesis, Characterization and Catalytic Oxidations of Oxovanadium(IV), Oxotitanium(IV) and Dioxomolybdenum(VI) Complexes with Chiral Imines of L-amino Acids

LUIGI CASELLA*, MICHELE GULLOTTI, ALESSANDRO PINTAR

Dipartimento di Chimica Inorganica e Metallorganica, Centro CNR, Università di Milano, Via Venezian 21, 20133 Milan, Italy

STEFANO COLONNA and AMEDEA MANFREDI

Dipartimento di Chimica Organica e Industriale, Centro CNR, Università di Milano, Via Golgi 29, 20133 Milan, Italy

(Received June 26, 1987)

Abstract

Representative oxovanadium(IV), oxotitanium(IV), and dioxomolybdenum(VI) complexes of *N*-salicylidene-L-amino acids (the amino acids are: valine, leucine, except for Mo(VI), and histidine) have been synthesized and characterized by various spectroscopic techniques. It has been found that while in the histidine complexes of titanium(IV) and vanadium(IV) the amino acid residue is bound in the expected glycine-like mode, in the molybdenum(VI) complex it is bound in the unusual histamine-like mode. Also, the structure of this molybdenum(VI) complex contains imidazolate-bridged polymeric units in the solid state, while the carboxyl group of the amino acid residue is protonated. In solution the polymeric structure is cleaved and the monomers contain carboxylate and protonated imidazole groups at the histidine residue. The histamine-like structure of the histidine complex was probed by comparison with that of the chiral dioxomolybdenum(VI) complex of *N*-salicylidene-L-histidinol. While the structure of the metal centers is six-coordinate for the dioxomolybdenum(VI) complexes and the histidine complexes of oxotitanium(IV) and oxovanadium(IV), it is likely that the complexes of the latter metals derived from nonpolar amino acids do not achieve coordination numbers higher than five. The present oxometal complexes are catalytically active in the sulfoxidation of sulfides and in the epoxidations of activated olefins by tert-butyl hydroperoxide, but in general exhibit a low degree of asymmetric induction in these reactions.

Introduction

Chiral transition metal complexes that can serve as catalysts for asymmetric synthesis are the subject of extensive investigation for the practical advantages offered by their use with respect to other synthetic methods. Catalytic asymmetric oxidations, in fact, usually proceed in mild conditions. Examples of such reactions are the catalytic hydrogenations with rhodium complexes containing chiral phosphine ligands [1], the asymmetric hydrosilylation and hydrocarbonylation [2a], the cross-coupling of Grignard reagents with Ni or Pd [2b], and the very recent use of $Ti(OPr^i)_4$, diethyl tartrate in the epoxidation of allylic alcohols [3a] and in the oxidation of organic sulfides [3b].

We have previously described in a series of papers a variety of zinc(II) [4, 5], copper(II) [5, 6], cobalt(II) [7], and iron(III) [8] complexes of the imines of L-amino acids and studied their stereochemical properties and reactions. Since transition metal complexes of group IVb, Vb, and VIb are well known for their ability to catalyze oxygen transfer reactions to for example sulfur atoms or olefinic double bonds [9], we thought it of interest to extend our investigation to the oxovanadium(IV), oxotitanium(IV), and dioxomolybdenum(VI) complexes with the same chiral ligands and to test their activity in catalytic oxidation reactions. Preliminary results described elsewhere [10] show that the oxotitanium(IV) complexes with the ligands H_2L^1 and H_2L^2 (Fig. 1) do in fact catalyze the asymmetric oxidation of sulfides to sulfoxides by tert-butyl hydroperoxide while the corresponding oxovanadium(IV) and dioxomolybdenum(VI) complexes are catalytically active but give no asymmetric induction. In this paper we describe the synthesis and characterization of the catalysts and some additional catalytic reactions performed by these systems.

Results and Discussion

Synthesis

We have synthesized the oxometal complexes of representative, tridentate ligands *N*-salicylidene-L-

*Author to whom correspondence should be addressed.

0020-1693/88/$3.50

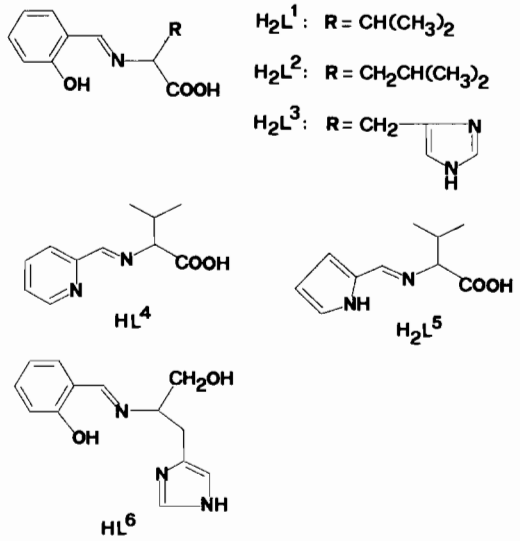

Fig. 1. Structure of the ligands.

amino acids containing relatively bulky, nonpolar side chains (H_2L^1 and H_2L^2) and the corresponding complexes derived from L-histidine (H_2L^3) where the imidazole group on the side chain can occupy an additional coordination position. We also prepared the dioxomolybdenum complexes of HL^4 and H_2L^5, to test eventual differences in catalytic activity originating from variation in donor set of the ligand and charge of the complex, and that of HL^6 in order to probe the coordination structure of MoO_2L^3. The molybdenum chelate derived from HL^4 contains acetylacetonate as anion, probably coordinated to the metal, the presence of which was confirmed by elemental analysis, IR and NMR spectra.

The complexes VOL^1 and VOL^2 have been known for some time [11] and we followed the same preparative procedure to obtain the histidine derivative VOL^3. The titanium(IV) and molybdenum(VI) complexes were routinely prepared by reacting the corresponding oxometal acetylacetonates with the partially preformed Schiff base ligand in aqueous–alcoholic medium at reflux temperature, followed by repeated evaporation of the solvent in order to remove free acetylacetone. Somewhat surprisingly, we could not obtain the complex MoO_2L^2 in pure form according to this preparative procedure or several variants of it. In all cases we isolated green paramagnetic materials with unsatisfactory analytical data. In addition, we found that when the reaction mixture of MoO_2L^3 was subjected to prolonged heating at reflux temperature as for the other complexes an analytically pure but completely optically inactive product was obtained. The elemental analyses of the complexes are collected in Table I.

IR Spectra

In general, the infrared spectra of the complexes display resolved imine ν(C=N) bands in the range 1620–1650 cm^{-1} flanked, at lower energy, by bands originating from aromatic ring vibration modes and carboxylate ν_{as}(COO) stretching (Table I). An unusual behavior is observed with the histidine complex MoO_2L^3; the broad and intense carboxylate band near 1600 cm^{-1} is clearly missing in its IR spectrum (the weak and sharp absorption observed at 1600 cm^{-1} is due to a ring vibration) and it is replaced by a very strong band at 1700 cm^{-1} that must be associated with a protonated carboxyl group. The presence of this group is confirmed by a sharp ν(OH) band at 3280 cm^{-1}. Since the elemental analysis excludes the presence of water and the complex is clearly diamagnetic (see below) we conclude that the dianionic ligand has undergone deprotonation at the imidazole NH group, rather than at the carboxyl group, on complex formation, to give oligomeric, imidazolate-bridged structures of type I. This

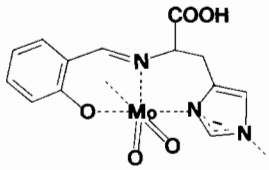

I

behavior is unusual in the coordination chemistry of histidine imines and is completely unexpected on the basis of the type of fused chelate rings present in the complex [4–8]. The somewhat low ν(C=O) and ν(OH) stretching frequencies observed probably result from intermolecular hydrogen bonding to support the oligomeric structure. The complex pattern of ν(Mo=O) vibrations near 900 cm^{-1} seems to confirm this hypothesis since these groups may also participate in hydrogen bonding. It is unfortunate that we could not obtain suitable crystals for a structural characterization of the complex but its low solubility in most common organic solvents represents a practical limitation in the attempts to crystallize this product. In donor solvents the imidazolate-bridged structure is apparently cleaved; in fact, the IR spectrum of MoO_2L^3 taken in solution of dry dimethylsulfoxide shows a broad and intense band at 1620 cm^{-1}, comprising the absorptions of the imine and carboxylate groups, while the 1700 cm^{-1} band is completely absent.

The IR spectra of other molybdenum complexes exhibit the two ν(Mo=O) bands expected for the *cis*-MoO_2 moiety [12]. At similar energies occur the characteristic ν(V=O) bands for the oxovanadium(IV) complexes. A reduction in the ν(V=O) frequency from 1000 to 970 cm^{-1} observed for the

TABLE I. Elemental Analyses (%) (calculated values in parentheses) and Selected Infrared Data (cm^{-1}) (Nujol mulls) for the Metal Complexes

Compound	C	H	N	ν(C=N)	ν(ring), ν_{as}(COO)	ν(M=O)
$TiOL^1 \cdot 1/4H_2O$	50.15 (50.10)	5.10 (4.75)	5.15 (4.90)	1620sh	1602, 1587, 1558, 1506	[c]
$TiOL^2 \cdot 2H_2O$	47.10 (46.60)	5.65 (5.70)	4.30 (4.20)	1624	1601, 1553, 1540, 1521	945[c]
$TiOL^3 \cdot 2H_2O$	43.05 (43.70)	4.00 (4.25)	11.95 (11.75)	1640	1600, 1550, 1521	910[c]
$VOL^1 \cdot H_2O$	[a]			1622	1600sh, 1550, 1521	995
$VOL^2 \cdot H_2O$	[a]			1628	1603, 1549, 1526	995
$VOL^3 \cdot 2H_2O$	43.45 (43.35)	3.80 (4.20)	11.20 (11.65)	1623	1600sh, 1530	970
MoO_2L^1	40.00 (40.35)	4.20 (3.70)	3.90 (3.90)	1624	1600, 1540	941, 909
MoO_2L^3	40.60 (40.55)	3.00 (2.90)	11.05 (10.90)	1631	1700[c], 1600, 1553	929, 914, 904, 890sh
$MoO_2L^4(acac) \cdot H_2O$ [b]	42.50 (42.75)	4.80 (4.70)	6.50 (6.25)	1627	1611, 1584[d], 1565, 1506[d]	945, 910, 902
$MoO_2L^5 \cdot 3H_2O$	31.70 (32.10)	4.35 (4.85)	7.05 (7.50)	1652	1610, 1588	937, 902
$MoO_2L^6Cl \cdot 2H_2O$	35.08 (35.19)	3.79 (4.09)	9.66 (9.47)	1632	1602, 1576	932, 909

[a]See ref. 11. [b]Acetylacetone = acacH. [c]See text. [d]Acetylacetonate bands.

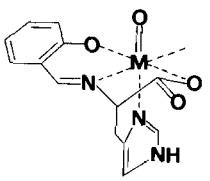

II

histidine complex VOL^3 can be accounted for by the weakening of the V=O bond on coordination of the imidazole group in the *trans* axial position (II).

Location of the Ti=O stretching frequency in the IR spectra of the titanium complexes is more difficult, since there are no prominent bands in the range expected for this vibration (900–1100 cm^{-1}) [13]. The spectrum of the histidine complex $TiOL^3$ displays a medium intensity band at 910 cm^{-1} that may be assigned to ν(Ti=O) but, in general, it is well known that titanium(IV) complexes containing a true titanyl moiety, Ti=O, are rarely found [14], while oligomeric species with μ-oxo bridges, Ti–O–Ti, usually prevail [15]. The pronounced IR absorptions near 800 cm^{-1} that we observe in the spectra of the present titanium complexes may in fact be due to μ-oxo Ti–O–Ti bridges [15].

Electronic and CD Spectra

The electronic and CD spectral data of the complexes are summarized in Table II. The very low solubility of most of the complexes in nondonor solvents limited markedly the range of solvents to be used in the investigation. The vanadyl complexes were studied in pyridine solution because it is known that these VO(IV) species are more stable in that solvent [16]. In general, a medium intensity absorption due to the low energy $\pi \rightarrow \pi^*$ transition of the salicylaldimine chromophore is clearly detectable as a separate band or a pronounced shoulder in the range 345–375 nm in the electronic spectra of the complexes. Corresponding bands occur in the CD spectra. For the vanadyl complexes three d–d bands of low intensity are detectable in the visible and near IR regions. Two of them can be observed in the CD spectra in the range covered by our instrument. Assuming an approximate C_{4v} symmetry and $^2B_2(xy)$ ground state, these bands can be assigned, in order of increasing energy, to the transitions $^2B_2(xy) \rightarrow {}^2E(xz, yz)$, $^2B_2(xy) \rightarrow {}^2B_1(x^2 - y^2)$ and $^2B_2(xy) \rightarrow {}^2A_1(z^2)$.

The optical activity of the imine band is important because it is related to the conformation of the amino acid chelate ring and, for the histidine complexes,

TABLE II. Electronic and CD Spectral Data for the Complexes

Compound	Solvent	UV λ_{max} (nm) (ϵ (dm^3 mol^{-1} cm^{-1}))	CD λ_{max} (nm) ($\Delta\epsilon$ (dm^3 mol^{-1} cm^{-1}))
$TiOL^1$	dimethylsulfoxide	296 (10250), 360sh (4100)	310 (−20.58), 360sh (−6.55), 398 (+4.67)
$TiOL^2$	dimethylsulfoxide	280sh (15000), 325sh (5900), 370sh (4000)	285 (−11.40), 340sh (−2.42), 390 (+4.51)
$TiOL^3$	dimethylsulfoxide	290sh (10500), 370sh (3500)	274 (+7.89), 301 (−4.42), 380 (−5.41)
VOL^1	pyridine	320sh (2100), 375 (2680), 525sh (48), 670 (22), 800sh (18)	368 (−2.61), 520 (−0.20), 660 (+0.24)
VOL^2	pyridine	310sh (2070), 375 (2730), 525sh (50), 720 (40), 830sh (35)	372 (−1.48), 513 (−0.16), 650 (+0.14)
VOL^3	pyridine	310sh (4075), 360 (2400), 405sh (1300), 520sh (130), 615sh (45), 860 (32)	383 (−5.37), 405sh (−4.30), 490 (−0.79), 596 (+1.38)
MoO_2L^1	methanol	266 (12400), 320sh (2300), 350sh (2030)	256 (+16.24), 302 (−2.13), 365 (+2.52)
MoO_2L^3	methanol	282 (11850), 345 (2700)	275 (−0.52), 315 (+0.26), 360 (−0.28)
MoO_2L^4(acac)	methanol	256 (9300), 293 (6900), 325sh (2700)	275 (−0.53), 315 (+0.66)
MoO_2L^5	methanol	285 (8380), 327 (14800)	265 (−0.74), 290sh (+0.65), 315 (+1.09), 340 (−0.22)
MoO_2L^6Cl	methanol	280sh (9700), 340 (2550)	279 (−11.31), 355 (−5.16)

also reflects the mode of chelation of the amino acid [4–8]. The observation of the imine CD band in the spectra of the titanium complexes is somewhat complicated by the presence of additional CD features near 400 nm that do not correspond to significant optical absorption and we believe originate from LMCT transitions. For $TiOL^1$ and $TiOL^2$ the 400 nm CD band is positive, while for $TiOL^3$ it is negative and largely overlaps with the imine band to give a single broad band. In general, however, for both the titanium and vanadium complexes it is clear that the chiroptical behavior of the histidine complexes parallels that of the complexes derived from amino acids with nonpolar side chains. This implies the adoption of the expected [4–8] glycine-like coordination mode by the histidine residue, as shown schematically by structure **II**.

For the molybdenum complex MoO_2L^3 it is of interest to establish whether the unusual histamine-like coordination mode of the histidine residue deduced from the solid-state IR spectrum of the complex is maintained in solution. The useful reference complexes are MoO_2L^1, where the amino acid residue is bound glycine-like, and the chiral complex MoO_2L^6Cl, derived from L-histidinol, where the amino alcohol residue is forced to chelate as a substituted histamine. The CD spectra clearly show the same pattern for MoO_2L^3 and MoO_2L^6Cl, while both these spectra bear a mirror image relationship with that of MoO_2L^1, thus confirming that in MoO_2L^3 the histidine residue retains the histamine-like mode of binding in solution.

The consistency of this picture is somewhat tempered by the intriguing observation that the CD behavior of the three salicylaldimine molybdenum complexes is just opposite to the established trend according to which we expect a negative imine band for MoO_2L^1 and a positive imine band for MoO_2L^3 and MoO_2L^6Cl [4–8]. The apparent contradiction is resolved by considering that, unlike the titanium and vanadium complexes, as well as all the previous series of salicylaldimine complexes of L-amino acids [4a, 6–8], the molybdenum complexes MoO_2L^1 and MoO_2L^3 racemize when dissolved in pyridine solution. The low optical stability of the histidine complex is confirmed by the ease with which it undergoes racemization during preparation. As we have occasionally observed for other imine complexes of amino acids, including histidine [6c, 17], this behavior can only be accounted for by assuming that the amino acid chelate ring adopts the conformation containing a pseudoequatorial side chain. This conformation implies a ring chirality which is opposite to that usually adopted by salicylaldimine complexes of amino acids and contains a pseudoaxial and hence easily removable proton [6c]. The histidinol complex MoO_2L^6Cl is optically more stable than the corresponding amino acid complexes, but this is quite certainly due to the replacement of the strong electron withdrawing carboxylate group at the α-CH position with the hydroxymethylene group.

The reasons for the peculiar behavior of the molybdenum complexes are difficult to assess precisely on the basis of the spectral data alone. We believe that the large size and tendency to six-coordination of the molybdenum complexes encourage binding of an additional donor ligand in the axial position *trans* to the oxo group. This is possible only if the amino acid side chain is pseudoequatorial, as shown schematically by structure **III**, while such a binding would be severely hindered by a pseudoaxial side chain, as in **IV**. The differences observed in the NMR spectra between MoO_2L^1 and $TiOL^1$, which has a structure corresponding to **IV**, support this interpretation. The donor ligand (S) can be a molecule of solvent or another donor group in an oligomeric

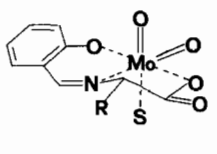

III

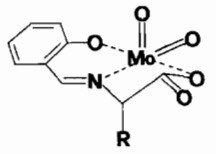

IV

structure. For MoO_2L^3, the preference for the histamine mode of binding is probably determined by the larger size and flexibility of the two fused, six-membered chelate ring system achieved by the ligand (**V**) with respect to the more rigid arrangement involved with the glycine-like binding mode shown in structure **II**. Note that the pseudoequatorial carboxylate group in **V** cannot coordinate intramolecularly to the metal center; though, it can obviously be involved in metal binding intermolecularly, in an oligomeric structure.

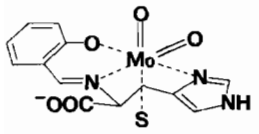

V

Like MoO_2L^3, MoO_2L^4(acac) and MoO_2L^5 also exhibit rather low optical activity. As shown by NMR, this is due to the presence of multiple species in solution. It should be noticed that for metal complexes derived from pyridine-2-carboxaldehyde the imine bands occur near 290 nm [5] and for those derived from pyrrole-2-carboxaldehyde they occur near 340 nm [18].

NMR Spectra

The proton NMR data for the diamagnetic complexes are collected in Table III. Unfortunately, the low solubility of the complexes $TiOL^2$ and especially $TiOL^3$ did not allow us to obtain sufficient resolution of the spectra for an accurate analysis. In general, the NMR spectra show imine proton signals in the range 8.5–9.0δ. These are broadened by long range couplings to the α-CH of the amino acid residue and the aromatic protons, where these couplings are much better resolved. Comparison of the spectra of the valine complexes $TiOL^1$ and MoO_2L^1 reveals opposite trends for the vicinal coupling constants between the α-CH and β-CH and the β-CH and the methyl groups. The value of $J_{\alpha\beta}$ for $TiOL^1$ is smaller than that observed for MoO_2L^1 and is also smaller than those found for free valine in a wide range of pH [19]. This is surprising since a lower value of $J_{\alpha\beta}$ may indicate an increased contribution of the rotational isomers with α-CH–β-CH protons in the gauche arrangement (**VI** or **VII**) with respect to the free amino acid, whereas the *trans* isomer (**VIII**) should be the more stable form of the complex on steric ground (structures **VI–VIII** are depicted assuming a pseudoaxial disposition of the side chain). We believe that the reduction in $J_{\alpha\beta}$ for $TiOL^1$ from the value of free valine results from the higher electronegativity of the metal-coordinated imine group with respect to NH_2 or NH_3^+, while the overall mobility of the side chain is probably not too different from that of the free amino acid. This interpretation seems supported by the finding that the coupling constant between the β-CH and the two methyl groups is similar to that found for the free amino acid [19].

TABLE III. Proton NMR Data for the Titanium(IV) and Molybdenum(VI) Complexes in Dry Dimethylsulfoxide-d_6 Solution[a]

Compound	CH=N	Ph–H	α-CH	β-CH	CH_3	Others
$TiOL^1$	9.06(~s)	6.6–8.0(m)	4.60(dd) [J_1 = 0.8 Hz; $J_{\alpha\beta}$ = 3.7 Hz]	2.0–2.4(m)	1.00(d), 1.08(d) [J_2 = 6.4 Hz][b]	
$TiOL^2$	8.98(~s)	6.6–8.0(m)	4.7(m)	1.5–2.5(m)[c]	0.8–1.0(m)	
$TiOL^3$	9.03(~s)	6.4–8.0(m)	4.5(m)	2.8–3.7(m)		8.32(~s)[d], 12.3[e, f]
MoO_2L^1	8.76(~s)	6.9–7.8(m)	4.20(dd) [J_1 = 1.3 Hz; $J_{\alpha\beta}$ = 5.8 Hz]	2.0–2.5(m)	1.00(d), 1.08(d) [J_2 = 4.7 Hz][b]	
MoO_2L^3	8.98(~s)	6.8–7.8(m)	5.18(m)[g] [J_1 = 1.0 Hz; $J_{\alpha\beta}$ = 2.6 Hz; $J_{\alpha\beta'}$ = 5.4 Hz]	3.0–3.6(m)[g] [$J_{\beta\beta'}$ = 16.5 Hz; J_3 = 1.1 Hz]		7.10(m)[h], 8.36(d)[d], 12.8(~s)[e, f] [J_4 = 1.3 Hz]
MoO_2L^4(acac)	8.56(m)[g]	7.3–8.2(m)[i]	4.2(m)	1.9–2.4(m)	0.85(d), 0.96(d) [J_2 = 6.8 Hz][b]	2.28(s)[j], 2.42(s)[j], 5.3[e, k]
MoO_2L^6Cl	8.64(~s)	6.8–7.6(m)	4.5(m)	3.2–3.6(m)		3.12(~d)[l], 4.42(~s)[m], 7.05(~d)[h], 8.29(~d)[d] [J_4 = 1.3 Hz; J_5 = 5.4 Hz]

[a]All shifts are given in ppm with reference to Me_4Si. $J_1 = J(CH{=}N,H_\alpha)$; $J_2 = J(CH_3,H_\beta)$; $J_3 = J(Im4\text{-}H,H_\beta)$; $J_4 = J(Im2\text{-}H,Im4\text{-}H)$; $J_5 = J(H_\alpha,CH_2OH)$. [b]The coupling to the β-CH proton is the same for the two methyl groups. [c]Including γ-CH. [d]Imidazole 2-H. [e]Broad. [f]Imidazole NH. [g]See text. [h]Imidazole 4-H. [i]Pyridine ring protons. [j]2,4-Pentanedionate methyl. [k]2,4-Pentanedionate CH. [l]CH_2OH. [m]OH.

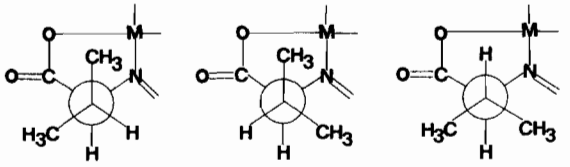

VI VII VIII

By contrast, for MoO_2L^1 the value of $J_{\alpha\beta}$ is much higher than that of the free amino acid, even though the higher formal positive charge of the metal should further increase the electronegativity effect of the imine group. The higher $J_{\alpha\beta}$ value indicates a more marked contribution of the *trans* rotamer (**XI**) at the conformational equilibrium (structures **IX–XI** are now depicted with a perspective emphasizing the pseudoequatorial disposition of the side chain, as suggested by the CD spectrum of the complex). The coupling between the β-CH and the methyl group is also affected, the marked reduction from the value observed for the free amino acid [or $TiOL^1$, or MoO_2L^4(acac)] reflects restricted mobility of the side chain of the valine fragment in MoO_2L^1. These data concur with the CD results and the chemical behavior of the molybdenum complexes to indicate that the form **XI** is stabilized because it produces the least amount of steric repulsion between the side chain and a nearby molecule of solvent (S) apically coordinated to the metal. With titanium, due to its smaller size, the access of an axial donor ligand is difficult even for the *trans* rotamer (**VIII** or **XI**); its behavior thus parallels that usually found for other complexes of this type, that do not generally achieve coordination number higher than five [4–8].

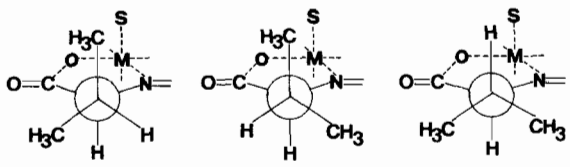

IX X XI

The NMR spectrum of the histidine complex MoO_2L^3 shows a signal at low field (12.8 δ) similar to that exhibited by $TiOL^3$ and assigned to the imidazole NH. This substantiates the IR data indicating that the oligomeric imidazolate-bridged structure of this complex found in the solid state is cleaved, at least in polar solvents, in favor of the traditional structure containing a deprotonated carboxyl group. The spectrum of the α-CH–β-CH_2 fragment shows a complex pattern of signals because long range couplings between the α-CH and the imine proton and the β-CH_2 and the imidazole 4-H proton give further splittings of the component of an ABX system. Though, the ABX pattern can be obtained by appropriate decoupling of the imine and imidazole 4-H protons. Analysis of this system [20] gave the geminal coupling constant $|J_{\beta\beta'}| = 16.5$ Hz (the sign of which must be negative) and the vicinal coupling constants $J_{\alpha\beta} = 2.6$ Hz and $J_{\alpha\beta'} = 5.4$ Hz, where β′ refers to the methylene proton resonating at higher field. Using these data it is possible to predict the dihedral angles between the two sets of H–C_α–C_β and C_α–C_β–H planes from the Karplus equation [21]. Although it may be dangerous to use this relationship indiscriminately, especially for metal complexes, the application of versions of the Karplus equation adapted to amino acid fragments [22] gave dihedral angles of 60°–70° for the α-CH–β-CH protons and 40°–50° for the α-CH–β′-CH protons. Inspection of molecular models shows that dihedral angles in these ranges can correspond to boat conformations carrying either pseudoaxial or pseudoequatorial carboxylate group. Such boat conformations were actually found in the only one structure available for a metal complex of histidine imines containing histamine-like chelate rings [17]. But we note that similar dihedral angles occur also in the glycine-like chelate structure of type **II**, while the comparison with the NMR data of MoO_2L^6Cl is of little utility, since the additional coupling of the α-CH proton to the hydroxymethylene protons in this compound makes the α-CH signal too complex for analysis. NMR is thus unable to discriminate between the various possibilities, unlike CD, which on the other hand gives information only about the dominant conformer in solution.

The NMR spectrum of MoO_2L^4(acac) shows the presence of two species in solution, as evidenced by the signals attributable to the imine, α-CH and acetylacetonate methyl protons. For MoO_2L^5 a broad signal at 13 δ indicates that the pyrrole ring nitrogen is protonated. In solution this complex must thus be formulated as MoO_2(HL)OH, but multiple species seem to exist, since the appearance of the NMR spectrum is very complicated (data not shown). The presence of various species in solution for both MoO_2L^4(acac) and MoO_2L^5 accounts for the low intensity of the CD spectra of these compounds.

TABLE IV. ESR Spectral Parameters for the Vanadium(IV) Complexes in Frozen Solution (−150 °C)

Compound	Solvent	$g_\perp$	$g_\parallel$	$A_\perp \times 10^{-4}$ (cm^{-1})	$A_\parallel \times 10^{-4}$ (cm^{-1})
VOL^1	methanol	1.987	1.957	61.9	171.1
	pyridine	1.986	1.960	57.2	164.7
VOL^2	methanol	1.985	1.956	64.0	167.3
	pyridine	1.986	1.960	58.5	164.9
VOL^3	methanol	1.987	1.960	59.3	164.9
		1.985	1.954	58.7	170.0
	pyridine	1.986	1.959	59.1	163.6
		1.984	1.951	58.7	167.4

ESR Spectra

The oxovanadium(IV) complexes are paramagnetic and gave well resolved ESR spectra. Typical axial ESR spectra were obtained from frozen samples in various solvents. The spin Hamiltonian parameters were calculated following the method described in ref. 23*; the results are collected in Table IV. For VOL^3 two species were clearly present and we have analyzed these spectra as a superposition of two axial spectra (Fig. 2). Coincident perpendicular lines had to be assumed for the two species because these lines were not resolved in the spectra. Therefore, the ESR spectral data for VOL^3 are less accurate than those of the other complexes.

The $g_\parallel$ and $A_\parallel$ values obtained for VOL^1 and VOL^2 are in the range expected for complexes with the present ligand donor atoms [23]. The change of solvent from methanol to pyridine shows a slight decrease of $A_\parallel$ and $A_\perp$, while the differences in $g_\parallel$ and $g_\perp$ are probably not significant, and agree with an increase of the in-plane ligand field strength of the solvent occupying the fourth equatorial coordination position. For VOL^3 the ESR data should represent the additional effect of an axial imidazole group but the existence of two species makes difficult the interpretation of this effect. The two species may be associated with isomers with different structure, monomer–dimer equilibria or species containing molecules of solvent coordinated and noncoordinated.

Catalytic Oxidations

The use of TiOL^1 and MoO_2L^1 as chiral catalysts has been extended to the epoxidation of 2-phenyl-*E*-cinnamyl alcohol (**XII**) with t-BuOOH. The same alcohol was employed by Sharpless and coworkers in the presence of $Ti(OPr^i)_4$ and diethyl tartrate [24]; therefore a comparison of the two procedures is straightforward. The degree of asymmetric induction was evaluated by comparison of the optical rotation of the epoxyacetate (**XIV**) with that of a true sample with known enantiomeric excess (e.e), as evaluated by ^{1}H NMR spectroscopy in the presence of an europium salt as chiral shift reagent. The TiOL^1 complex is more efficient than MoO_2L^1 in the formation of the epoxy derivative (**XIV**) as far as the chemical yields are concerned, but it is less stereoselective: 9% e.e. *versus* 15% e.e., respectively. These results, however, are far from those obtained by Sharpless (e.e. $\geqslant$ 95%).

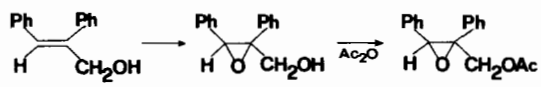

XII **XIII** **XIV**

The activation of the double bond by the hydroxyl group towards the electrophilic attack by the oxidant is essential, since alkenes not functionalized such as 1-methyl cyclohexene in the usual reaction conditions with either TiOL^1 or MoO_2L^1 as catalysts are recovered unchanged after a long reaction time. On the other hand the Weitz–Scheffer epoxidation of 2-phenyl-1,4-naphthoquinone (**XV**) with t-BuOOH and solid NaOH in the presence of TiOL^1 as catalyst leads to the epoxide (**XVI**) with good chemical yields (60%) but low e.e. (2.6%) as indicated by its ^{1}H NMR spectra in the presence of $Eu(dmc)_3$ as chiral shift reagent. These results as a whole show the versatility of the oxometal complexes of *N*-salicylidene-L-amino acids as catalysts for oxidation reactions, since they apply, in appropriate conditions, to the sulfoxidation of organic sulfides and the epoxidation of electron poor and

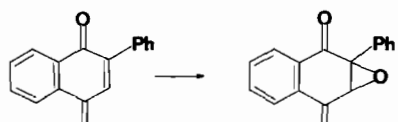

XV **XVI**

*Some of the equations reported in ref. 23 (p. 71, 72) for the iterative calculation procedure of the ESR spectral parameters are incorrect. The set of equations that we used are as follows:

$$A_\parallel = \left[g_\parallel \beta(H_{m_{2\parallel}} - H_{m_{1\parallel}}) + \frac{A_\perp^2}{2\nu_0}(m_{1\parallel}^2 - m_{2\parallel}^2) \right] \Big/ (m_{2\parallel} - m_{1\parallel})$$

$$g_\parallel = \left\{ 2\nu_0 + A_\parallel(m_{2\parallel} + m_{1\parallel}) - \frac{A_\perp^2}{\nu_0} \left[I(I+1) - \frac{(m_{2\parallel}^2 + m_{1\parallel}^2)}{2} \right] \right\} \Big/ \beta(H_{m_{2\parallel}} + H_{m_{1\parallel}})$$

$$A_\perp = \left[g_\perp \beta(H_{m_{2\perp}} - H_{m_{1\perp}}) + \frac{(A_\perp^2 + A_\parallel^2)}{4\nu_0}(m_{1\perp}^2 - m_{2\perp}^2) \right] \Big/ (m_{2\perp} - m_{1\perp})$$

$$g_\perp = \left\{ 2\nu_0 + A_\perp(m_{2\perp} + m_{1\perp}) - \left(\frac{A_\perp^2 + A_\parallel^2}{2\nu_0} \right) \left[I(I+1) - \frac{(m_{2\perp}^2 + m_{1\perp}^2)}{2} \right] \right\} \Big/ \beta(H_{m_{2\perp}} + H_{m_{1\perp}})$$

where $H_{m_{2i}}$ and $H_{m_{1i}}$ (i = $\parallel$ or $\perp$) are the resonance fields of any two parallel or perpendicular lines, m_{2i} and m_{1i} ($m_{2i} > m_{1i}$), β is the Bohr magneton, ν_0 is the spectrometer frequency, and I is 7/2 for ^{51}V.

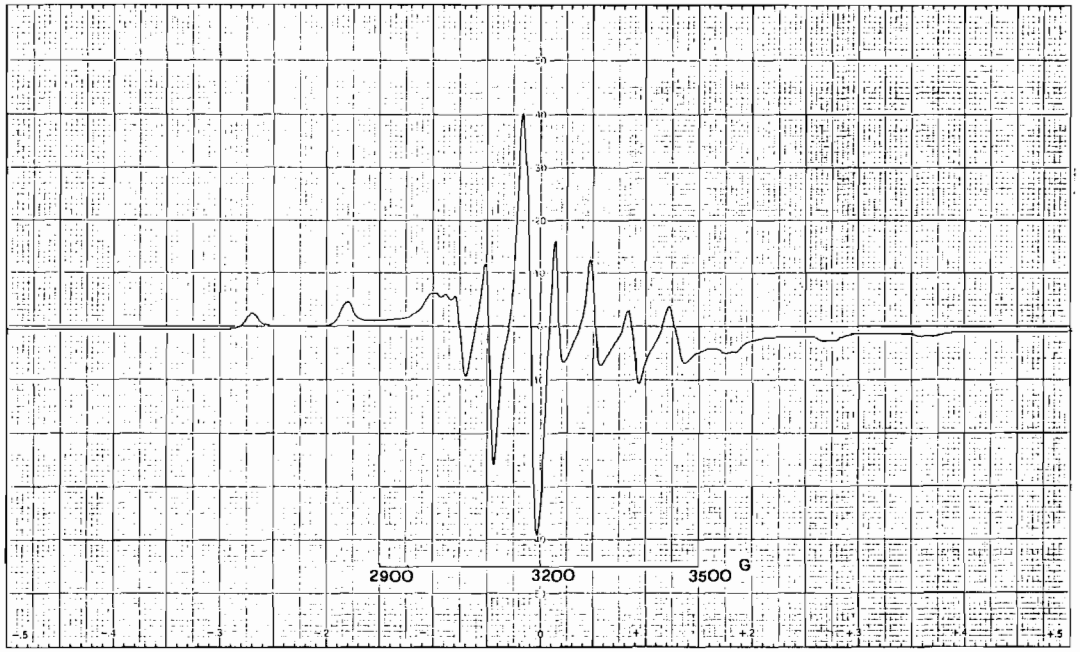

Fig. 2. ESR spectrum of VOL^3 in frozen pyridine solution at −150 °C.

electron rich olefins; however, the scarce or weak interactions with the substrates [10] leads to modest asymmetric induction.

Experimental

Physical Measurements

Elemental analyses were from the microanalytical laboratory of the University of Milano. Electronic spectra were recorded on a Perkin-Elmer Lambda-5 spectrophotometer and circular dichroism spectra on a Jasco-500 C dichrograph. Infrared spectra were recorded on a Nicolet MX-1E FT-IR instrument. Electron spin resonance spectra were recorded on a Varian E-109 instrument operating at X-band frequencies. Proton NMR spectra were recorded on Bruker WP-80 and AC-200 FT spectrometers.

Preparations

The oxovanadium(IV) complexes were prepared according to a literature procedure [11]. The oxotitanium(IV) and dioxomolybdenum(VI) complexes were prepared by refluxing for 0.5 h or, in the case of L-histidine, simply warming for a few minutes (to prevent cyclization of the Schiff base [4a]), the amino acid (5 mmol) and the aldehyde (5 mmol) in 50 ml of methanol–water (1:1, *v/v*), and then adding solid $TiO(acac)_2$ or $MoO_2(acac)_2$ (5 mmol) to the solution of the partially preformed Schiff base. The mixture was refluxed for a few hours, except for MoO_2L^3, which was treated overnight under stirring at room temperature. Then the mixture was taken to dryness several times from ethanol–water (1/1, *v/v*) under reduced pressure, in order to eliminate free 2,4-pentanedione. The solid residue was treated with methanol under stirring, filtered, washed with alcohol and then dried under vacuum. In the case of $TiOL^3$ the material isolated contained a little amount of TiO_2. This was eliminated by dissolving the complex in pyridine and filtering off the white, insoluble powder. The complex was then recovered by evaporation to dryness of the filtrate and treatment of the residue with ethanol, followed by filtration and drying under vacuum. The elemental analyses of the complexes are collected in Table I.

Catalytic Oxidations

The epoxyacetate (**XIV**) was prepared according to the literature [24], by reaction of the corresponding crude epoxide (**XIII**) with Ac_2O and pyridine in anhydrous benzene as solvent and purified by column chromatography (light petroleum–diethyl ether 7/3, *v/v* as eluant). The starting epoxide (**XIII**) was obtained, in turn, by reacting the allylic alcohol (1 mmol) with MoO_2L^1 or $TiOL^1$ (0.1 mmol) in anhydrous benzene (10 ml) with anhydrous t-BuOOH 1.9 M (1 mmol) for 18 h, and 144 h, respectively. The chemical yields into the epoxyacetate was 22%, with MoO_2L^1 as catalyst, n_D^{20} 1.5517, $|\alpha|_D^{25} = -6.9°$ (c 0.8 in CCl_4), whereas with $TiOL^1$ it was 70%, $|\alpha|_D^{25} = +3.9°$ (c 1.7 in CCl_4), the e.e. being 15.7% and 9.0%, respectively.

The epoxidation of 2-phenyl-1,4-naphthoquinone (**XV**) was performed by reacting the quinone (1 mmol) in anhydrous benzene (10 ml) with $TiOL^1$ (0.1 mmol) and anhydrous t-BuOOH 1.96 M (1 mmol) in

the presence of solid NaOH (0.25 mmol) for 3 h. The reaction mixture was washed with aqueous Na_2SO_3, the organic layer was separated and extracted with diethyl ether. The combined organic phases were washed with water, dried with $MgSO_4$ and evaporated under vacuum. The crude product was purified by column chromatography (SiO_2, light petroleum–diethyl ether 95/5, *v/v*, as eluant) to afford epoxide **(XVI)** in 5.6% yield, n_D^{28} 1.6759, $|\alpha|_D^{25} - 1.93°$ (~1.9 in $CHCl_3$), e.e. 2.6%.

Acknowledgements

This work was supported by the Italian CNR. We thank Professor P. Fantucci for writing the program for the ESR spectra calculation and M. Bonfà for recording the NMR spectra.

References

1 H. B. Kagan, in G. Wilkinson, F. G. A. Stone and E. W. Abel (eds.), 'Comprehensive Organometallic Chemistry', Vol. 8, Pergamon, Oxford, 1982, p. 463.
2 (a) I. Ojima and K. Hirai, in J. D. Morrison (ed.), 'Asymmetric Synthesis. Vol. 5. Chiral Catalysis', Academic Press, Orlando, 1985, p. 104; (b) S. Otsuka and K. Tani, p. 171.
3 (a) M. G. Finn and K. B. Sharpless, in J. D. Morrison (ed.), 'Asymmetric Synthesis. Vol. 5. Chiral Catalysis', Academic Press, Orlando, 1985, p. 247; (b) C. Puchot, O. Samuel, E. Dunach, S. Zhao, C. Agauni and H. B. Kagan, *J. Am. Chem. Soc., 108,* 2353 (1986).
4 (a) L. Casella and M. Gullotti, *J. Am. Chem. Soc., 103,* 6338 (1981); (b) *105,* 803 (1983); (c) L. Casella, M. Gullotti and A. Rockenbauer, *J. Chem. Soc., Dalton Trans.,* 1033 (1984).
5 L. Casella and M. Gullotti, *Inorg. Chem., 22,* 2259 (1983).
6 (a) L. Casella, M. Gullotti, A. Pasini and A. Rockenbauer, *Inorg. Chem., 18,* 2825 (1979); (b) L. Casella and M. Gullotti, *Inorg. Chem., 20,* 1306 (1981); (c) L. Casella, M. Gullotti and G. Pacchioni, *J. Am. Chem. Soc., 104,* 2386 (1982); (d) L. Casella, M. Gullotti and E. Melani, *J. Chem. Soc., Perkin Trans. I,* 1827 (1982).
7 L. Casella and M. Gullotti, *Inorg. Chem., 25,* 1293 (1986).
8 L. Casella, M. Gullotti, A. Pintar, L. Messori, A. Rockenbauer and M. Györ, *Inorg. Chem., 26,* 1031 (1987).
9 (a) R. A. Sheldon and J. K. Kochi, 'Metal-Catalyzed Oxidations of Organic Compounds', Academic Press, New York, 1981; (b) R. A. Sheldon, *Aspects Homogeneous Catal., 4,* 3 (1981); (c) H. Mimoun, *Angew. Chem., Int. Ed. Engl., 21,* 734 (1982); (d) H. Mimoun, *Isr. J. Chem., 23,* 451 (1983).
10 S. Colonna, A. Manfredi, M. Spadoni, L. Casella and M. Gullotti, *J. Chem. Soc., Perkin Trans. I,* 71 (1987).
11 L. J. Theriot, G. O. Carlisle and H. J. Hu, *J. Inorg. Nucl. Chem., 31,* 2841 (1969).
12 E. I. Stiefel, *Prog. Inorg. Chem., 22,* 1 (1977).
13 (a) J. Selbin, *Angew. Chem., Int. Ed. Engl., 5,* 712 (1966); (b) N. S. Biradar and S. D. Angadi, *Monatsh. Chem., 109,* 1365 (1978).
14 R. J. H. Clark, 'The Chemistry of Titanium and Vanadium', Elsevier, Amsterdam, 1968.
15 (a) T. Roberie and J. Selbin, *J. Coord. Chem., 9,* 89 (1979); (b) S. K. Pandit, S. Gopinathan and G. Gopinathan, *J. Less-Common Met., 64,* 163 (1979); (c) K. Wieghardt, U. Quilitzsch, J. Weiss and B. Nuber, *Inorg. Chem., 19,* 2514 (1980); (d) R. C. Fay, *Coord. Chem. Rev., 37,* 9 (1981); (e) M. Gullotti and A. Pasini, *Inorg. Chim. Acta, 15,* 129 (1975).
16 J. J. R. Frausto da Silva, R. Wootton and R. D. Gillard, *J. Chem. Soc. A,* 3369 (1970).
17 L. Casella, M. E. Silver and J. A. Ibers, *Inorg. Chem., 23,* 1409 (1984).
18 L. Casella, M. Gullotti, C. Pessina and A. Pintar, *Gazz. Chim. Ital., 116,* 41 (1986), and refs. therein.
19 J. J. M. Rowe, J. Hinton and K. L. Rowe, *Chem. Rev., 70,* 1 (1970).
20 E. D. Becker, 'High Resolution NMR Theory and Chemical Applications', Academic Press, New York, 1980, Chap. 7.
21 M. Karplus, *J. Chem. Phys., 30,* 11 (1959).
22 (a) R. J. Abraham and K. A. McLauchlan, *Mol. Phys., 5,* 513 (1962); (b) R. J. Weinkam and E. C. Jorgensen, *J. Am. Chem. Soc., 95,* 6084 (1973); (c) C. De Marco, M. Llinàs and K. Wüthrich, *Biopolymers, 17,* 617 (1978); (d) J. Feeney, *J. Magn. Reson., 21,* 473 (1976).
23 N. D. Chasteen, in L. J. Berliner and J. Reuben (eds.), 'Biological Magnetic Resonance', Vol. 3, Plenum, New York, 1981, p. 53.
24 R. C. Michaelson, R. E. Palermo and K. B. Sharpless, *J. Am. Chem. Soc., 89,* 1990 (1977).